

# Decay width of light quark hybrid meson from the lattice.

C. McNeile and C. Michael  
*Theoretical Physics Division, Dept. Math. Sci.,  
University of Liverpool, Liverpool L69 7ZL, UK.*

Lattice QCD with  $N_f = 2$  flavours of sea quark is used to explore the spectrum and decay of a  $J^{PC} = 1^{-+}$  spin-exotic hybrid meson. We test lattice determination of S-wave decay amplitudes at threshold using  $b_1 \rightarrow \pi\omega$  where agreement with data is found. We find a hybrid meson state at 2.2(2) GeV with a partial width to  $\pi b_1$  of 400(120) MeV and to  $\pi f_1$  of 90(60) MeV.

PACS numbers: 12.38.Gc, 12.39.Mk, 13.30.Eg

## I. INTRODUCTION

QCD has the potential to produce spin-exotic hybrid mesons. Lattice QCD is one of the most reliable ways to evaluate their properties and mass values have been reported. For a successful experimental study of such states, it is necessary that the total decay width is not too wide. The strength of this decay in which a gluonic excitation produces a quark-antiquark pair is not easy to estimate phenomenologically. For the case of heavy-quark hybrid mesons, lattice QCD has given guidance on the predominant decay channel and the decay width. This estimate [1] is of a width sufficiently narrow that experimental study is feasible. Here we address the issue of the decay mechanism and associated widths for the spin-exotic meson made of light valence quarks.

Lattice QCD offers a first principles route to determine the spectrum of spin-exotic hybrid mesons. The first reported results, refs. [2, 3, 4, 5], used quenched lattices. There have been subsequent studies using lattices with dynamical quarks, refs. [6, 7], but then the issue of the decay of the hybrid meson has to be addressed directly. Indeed the MILC group [7] emphasise that they cannot easily distinguish a hybrid meson from a two-body state such as  $\pi b_1$  with the same quantum numbers.

This is an important field to explore, since experimental results are somewhat inconclusive and there have been several candidate states proposed, see refs. [8, 9, 10, 11, 12, 13, 14, 15, 16].

The study of hadronic decays from the lattice is not straightforward - see ref. [17]. It is possible, however, to evaluate the appropriate hadronic matrix element from a lattice if the transition is approximately on-shell. Since we will explore S-wave decays at threshold, we test our lattice methods on a case which is known experimentally, namely  $b_1 \rightarrow \pi\omega$ , obtaining agreement. For the case of a spin-exotic hybrid meson (here we focus mainly on the isovector  $J^{PC} = 1^{-+}$  meson labelled  $\hat{\rho}$  where the ‘hat’ notation implies opposite C), the S-wave decays to  $\pi b_1$  and  $\pi f_1$  are explored here. We follow methods generically similar to those used by us to study  $\rho$  decay [18]. Indeed these methods were first employed [1] in a study of hybrid meson decay, where the valence quarks are taken as very heavy (i.e. static). Here we use light valence quarks - lighter than the strange quark.

## II. LATTICE METHODS

In order to study spin-exotic hybrid mesons, it is inevitable that non-local operators have to be used to create (and destroy) the hybrid meson - since hybrid mesons with spin-exotic quantum numbers explicitly cannot be made from quark and antiquark alone. The gluonic component can be incorporated either by using a closed colour flux loop (eg. clover-like) or by separating the quark and antiquark sites by a combination of colour flux paths. Here we use that latter construction - as it was found to be effective in an earlier study [2, 3].

In order to construct the hybrid meson sources, one needs either propagators from different spatial points [2], or some more elaborate construction. The hybrid meson is relatively heavy, so the signal to noise ratio will be poor. This suggests that a spatial-volume source would be attractive. Such sources are achievable using stochastic methods - and were indeed employed in our study of  $\rho$  decay [18]. Compared to the case of the  $\rho$  meson, the hybrid meson is even more challenging. We explored a variety of different prescriptions, attempting to optimise the signal/noise for the two-point hybrid correlator at moderate  $t$ -separations.

### A. Stochastic method

For a given effort (namely number of inversions), the stochastic noise is reduced the more one dilutes (or thins - see refs. [19, 20]) the set of stochastic sources used - until with sources at one colour-spin at one point, one has the conventional exact inversion. Conversely, the more correlators one evaluates, the more the statistical noise inherent in the gauge configurations is reduced. So clearly we have to compromise - and the balance point for a hybrid meson may be different from that used, for example, for  $\rho$  decay.

As an example, we measured the connected meson two-point correlator at  $t = 8$  from different methods using 200 gauge configurations (lattice U355 of Table I). The standard deviations over gauges were found to be for the  $b_1$  and  $a_0$  meson 0.0028 and 0.0125, respectively, from the conventional method using 12 colour-spin sources at one space-time site; 0.0015 and 0.0070 from using the

same conventional method with four space-time sources per gauge configuration; while with a stochastic spatial-volume source we obtained 0.0013 and 0.0034. The stochastic method is superior, especially for the  $a_0$  meson, although it involves more inversions as the method used a sequence of sources, each at one time value and one colour-spin value but all space. With 8 time values selected per gauge configuration, this involves  $12 \times 8$  inversions. The essential step in obtaining a small stochastic error is to minimise the number of random numbers needed to evaluate the relevant correlators. This we explain in more detail.

With a random source,  $\xi_i$ , which is non-zero on some subset of colour-spin-space-time and satisfies  $\langle \xi_i^* \xi_j \rangle = \delta_{ij}$ ;  $\langle \xi_i \xi_j \rangle = 0$  when averaged over different instances of the random numbers, then one solves the propagation from this source iteratively, as usual,  $M_{ik} \phi_k = \xi_i$ . Here we use Z2 noise in both real and imaginary parts. The basic idea is then that  $\xi_k^* \phi_j$  is an unbiased stochastic estimator of the propagator  $M_{jk}^{-1}$ , albeit a rather noisy one, and can be used to construct mesonic correlators. A considerable decrease in the noise comes from using the ‘one-end-trick’ which is [18, 19] to combine two appropriately related  $\phi$ ’s to obtain the mesonic two-point correlator. So if  $M_{ik} \phi_k^\Gamma = \Gamma_{ij} \xi_j$ , then  $\phi^{*\Gamma} \phi$  will, averaged over stochastic samples, automatically select a meson created by  $\bar{q} \Gamma q$ . An appropriate sum also needs to be made over the sink (indices available on  $\phi^\Gamma$  and  $\phi$ ) to destroy such a meson. If one uses random sources  $\xi$  for each spin component separately, one has the appropriate  $\phi^\Gamma$  available for any independent  $\gamma$  matrix or product of them. This is then an efficient method to evaluate all mesons created by  $\bar{q} \Gamma q$ , and we presented some results for the  $b_1$  and  $a_0$  two-point functions above.

In order to extend this approach to create a hybrid meson, one needs to create a source  $H_{ij} \xi_j$  for each original source  $\xi_i$  where  $H_{ij}$  is a sum of a set of operators comprising spatial paths and  $\gamma$ -matrices which create the hybrid meson when combined as above. In this work we only create the spin-exotic  $J^{PC} = 1^{-+}$  meson in one spin component. We also create a fuzzed source  $F_{ij} \xi_j$  to give us an independent mesonic creation operator. From  $\phi^{*H} \phi$  and  $\phi^{*H} \phi^F$ , we are able to create a hybrid meson in two different ways (the latter has some unwanted mixing of opposite C, which can be projected out by building the sink operator with the required C-value). We also need an extended propagator to cope with the pion emission in the decays we shall study. Thus overall we need  $4 \times 12 \times 8$  inversions per gauge configuration. This relatively heavy overhead is justified because with dynamical fermions, there are a limited set of gauge configurations.

## B. Lattice configurations and two point correlators

We wish to use gauge configurations with dynamical quarks so that decay is physically allowed, as in the real world. It is sufficient for this study to have  $N_f = 2$

flavours of sea-quark, since this allows the light quark sector to be explored. We use clover-Wilson fermions and the lattice data sets used are described in Table I. They have different quark masses and spatial volumes to explore systematic effects.

Because of the improved signal to noise offered by our stochastic method, we have improved determinations of the meson masses from two-point correlators. As well as local operators, we use fuzzing [21] with paths of length  $f_1$  ( $2a$  for U355 for compatibility with previous work,  $3a$  for C410) composed of fuzzed links (5 iterations of fuzzing with 2.5 straight + sum U-bends, projected to SU(3)). We have a  $2 \times 3$  matrix of correlators: local or fuzzed at the source and an additional larger scale fuzzing at the sink with fuzzed links with 10 iterations of fuzzing combined to length  $f_2$  ( $4a$  for U355,  $5a$  for C410). For the axial mesons  $b_1$  and  $a_1$ , we use operators  $\bar{q} \gamma_i \gamma_5 \gamma_4 q$  and  $\bar{q} \gamma_i \gamma_5 q$ , respectively, (and their fuzzed extensions) to determine the correlators which are fitted to give the ground state masses listed in Table II.

We are also able to extract the spin-exotic hybrid mass from our two-point correlators. We use a hybrid operator made (as in ref [2]) of U-shaped paths  $P_i$  from fuzzed links and combined with  $\gamma$ -matrices to be in the  $T_1^{-+}$  representation:  $\bar{q} \epsilon_{ijk} P_i \gamma_j q$ . We have at the source such an operator with sides of length  $f_1$  and also the fuzzed version of this (with straight links of length  $f_1$  combined with the U-shaped ones). At the sink we have both of these operators as well as an additional one made of U-shaped paths with length  $f_2$  composed of more heavily fuzzed links. At the sink we take care to give the fuzzed-hybrid operator a well defined charge conjugation. We again have a  $2 \times 3$  matrix of correlators which we fit to determine the energy eigenstates. Using the  $t$ -range 2-8, we obtain the mass values given (for the ground state) in Table II from a factorising fit to the correlator matrix with ground state and 1 excited state. The fit is illustrated in fig. 1 for U355. We can also use a  $2 \times 2$  submatrix of correlators in a variational treatment, obtaining  $m(\hat{\rho})a = 1.38(12)$  (U355 from  $t$ -values 5/4 with basis 3/2) and  $1.68(13)$  (C410 from  $t$ -values 4/3 with basis 3/2). These latter values are formally upper limits. They are consistent with the fitted values given in Table II.

To compare these mass determinations, we use  $r_0$ , obtaining  $m(\hat{\rho})r_0 = 7.0(3)$  and  $5.4(2)$  for U355, C410 respectively, where the errors are statistical only. There are also systematic errors from the fits, which can be constrained partly by the variational results quoted above, and which are at least as big as the statistical errors. These fit values are statistically barely consistent: it may be that finite volume effects are significant (C410 has a spatial extent 5/3 bigger than U355) or that finite lattice spacing effects are important (U355 has a smaller lattice spacing by 3/5 and uses NP clover rather than tadpole-improved clover). Since we are unable to distinguish between these scenarios, we construct a weighted average, namely:  $m(\hat{\rho})r_0 = 5.9(6)$ .

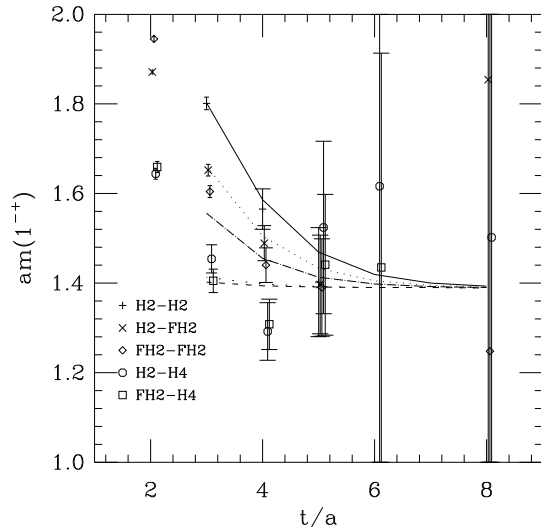


FIG. 1: Effective mass (from  $t : (t - a)$ ) of the  $J^{PC} = 1^{-+}$  hybrid meson in lattice units from a  $2 \times 3$  matrix of correlators for U355. The fit described in the text is illustrated.

We note that the result of previous quenched calculations was summarised [22] at around 1.9 GeV which corresponds to  $m(\hat{\rho})r_0 = 4.8$ . Thus we conclude that the  $N_f = 2$  studies, using a fully unitary theory, tend to give higher hybrid meson masses than quenched. Our averaged mass corresponds to 2.2(2) GeV (from  $r_0 = 0.53$  fm). As discussed later, there are additional systematic errors.

We also have measured correlators between two-body operators and the hybrid meson - these we will discuss in the context of the decay mechanism. They can also be used to extract energy values, as we discuss later. First we analyse the reliability of the evaluation of decay transition strengths for S-wave decays at threshold by considering a case where the result is known experimentally:  $b_1 \rightarrow \omega\pi$ .

### C. Transition $b_1 \rightarrow \omega\pi$

The study of decays from Euclidean lattice gauge theory has a long history and not many results. The only case that has been studied in detail on a lattice [18] where experimental results exist is  $\rho \rightarrow \pi\pi$  which has a P-wave decay, necessitating non-zero momentum on a lattice. For an S-wave decay, a zero momentum transition is accessible and this we explore here.

Code	no.	$\kappa$	$m(\pi)r_0$	$L/r_0$	$am(\pi)$	$am(\rho)$	
U355	200	0.1355	1.47	3.2	0.292(2)	0.491(7)	
C410	237	0.1410	1.29	5.3	0.427(1)	0.734(4)	
U395	12	20	0.1395	1.92	3.5	0.558(8)	0.786(8)
U395	16	20	0.1395	1.94	4.65	0.564(3)	0.785(8)

TABLE I: Lattice gauge configurations U355 from UKQCD [23], C410 from CP-PACS [24] and U395 from UKQCD [25] used. These have  $N_f = 2$  flavours of sea quark and we use valence quarks of the same mass as the sea quarks.

Code	$am(b_1)$	$am(a_1)$	$am(\hat{\rho})$
U355	0.78(2)	0.72(2)	1.39(6)
C410	1.17(3)	1.15(2)	1.78(5)

TABLE II: Axial meson and hybrid meson masses determined from lattice gauge configurations U355 and C410 using stochastic methods.

On a lattice, one can create two body states of a given total momentum. In a large spatial volume, these two bodies will interact very little and so the two body state will be approximately the product of the single body states. The interaction can be studied by measuring the shift in the two-body energy while varying the lattice spatial size, as established by Lüscher [26, 27, 28, 29]. This approach, however, needs very accurate energy determinations and is thus not feasible in many cases at present. A simpler, but less rigorous, alternative is to measure the transition strength from initial state to two-body state directly on a lattice. This is feasible [1] when the initial and final state have approximately the same energies (i.e. on-shell transition). The decay transition amplitude measured on a lattice can then be related to the large volume value via Fermi's golden rule. For an S-wave decay at threshold, the phase space is actually zero, so relating the lattice with a discrete spectrum of two-body states to the large volume continuum of two-body states needs to be validated.

Here we study  $b_1 \rightarrow \omega\pi$  which has predominantly an S-wave decay [30] with partial width  $\Gamma = 0.142(9)$  GeV. We shall compare effective coupling constants for the S-wave transition, defining  $\bar{g}^2 = \Gamma/k$  where  $k$  is the decay momentum, so  $\bar{g}^2 = 0.38(2)$ . In order to study the  $b_1 \rightarrow \omega\pi$  D-wave transition which would shed light on the decay mechanism [31], we would have to create non-zero momentum mesons which we do not study in this work.

On our lattices, the  $b_1$  mass is approximately the same as the sum of  $\pi$  and  $\rho$  masses, so we are close to an on-shell transition. In principle, the  $\omega$  meson, which is flavour singlet, receives disconnected contributions, but these we expect [32] to be negligible based on previous lattice studies. We measure the three-point correlation  $(b_1|\omega\pi)$  where the  $\pi$  and  $\omega$  are both summed over the

whole volume at one time-slice and the  $b_1$  meson is also summed over all volume at another time-slice. We measure for each of the three spin orientations of  $b_1$  and  $\omega$  (which are aligned). This is achieved using our stochastic methods with the  $\omega$  as the source and with an extended propagator for the zero-momentum pion, for which a fuzzed operator is chosen.

We then evaluate the ratio

$$R(t) = \frac{(b_1|\omega\pi)}{\sqrt{(b_1|b_1)(\omega|\omega)(\pi|\pi)}}$$

where each correlation is taken at the same  $t$ -separation on the lattice. This ratio  $R(t)$  of the three point correlation to a combination of two-point correlations normalises the meson creation operators. It is plotted in fig. 2 for the case where each meson operator is fuzzed (which enhances the ground state contributions). The slope of  $R$  versus  $t$  is then the lattice transition amplitude  $xa$ . We see that a linear behaviour is present over a significant interval in  $t$ , so confirming the interpretation of the slope as the lattice transition amplitude. In our further analysis, we evaluate this slope around  $t/r_0 = 1$ . The decay width  $\Gamma$  is then given, via Fermi's Golden Rule, by  $\Gamma/k = \bar{g}^2$ , where

$$\bar{g}^2 = \frac{1}{\pi}(xa)^2(L/a)^3 \frac{E(\omega)aE(\pi)}{E(\omega) + E(\pi)}$$

where  $k$  is the centre of mass momentum of the decay products.

The coupling strength  $\bar{g}^2$  should be independent of lattice spatial size ( $L$ ). Moreover its dependence on the quark mass can also be explored. In order to investigate, we evaluate the effective coupling from a range of different lattice configurations (all having  $N_f = 2$  flavours of sea-quark). We plot in fig. 3 the effective coupling  $\bar{g}$  evaluated from the slope ( $xa$ ) in fig. 2 at  $t/r_0 = 1$ .

For a zero-momentum transition, which is what we study here, there should be no dependence on lattice volume of the hadronic transition strength. In order to be able to vary the lattice spatial volume while keeping everything else fixed, we make use of  $12^3 \times 24$  and  $16^3 \times 24$  configurations labelled U395 in Table I. As shown on fig. 2, where the appropriate factor of  $(12/16)^{3/2}$  has been included,  $R(t)$  agrees within statistical errors for these two cases. This confirms that the extraction of the hadronic transition amplitude is insensitive to the lattice spatial volume when it is changed by a factor of 2.4.

To study the dependence on the quark mass, we compare our higher statistics studies U355 ( $m(\pi)r_0 = 1.47$ ) and C410 ( $m(\pi)r_0 = 1.29$ ). Qualitatively, we see from fig. 2, they have similar transition strengths. There is some evidence of a decrease of the coupling strength as the quark mass is decreased. This is consistent with approaching the experimental value as  $m(\pi) \rightarrow 0$ , as shown in fig. 3.

Thus we conclude that our method for extracting an estimate of the decay transition strength is indeed reli-

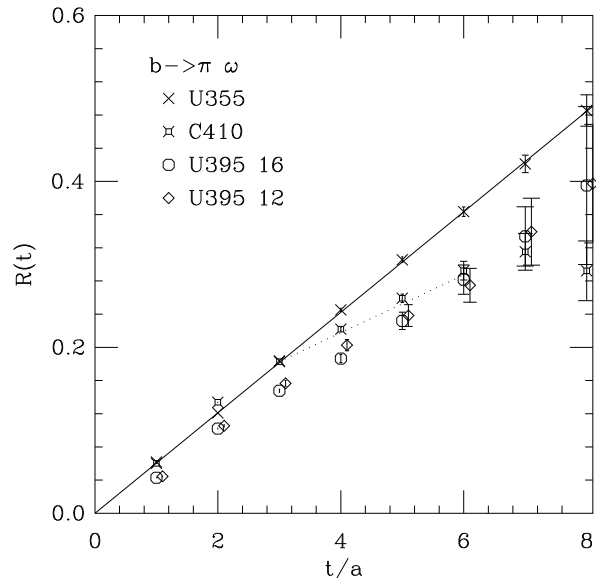


FIG. 2: Normalised ratio  $R(t)$  of transition  $b_1 \rightarrow \pi\omega$  at time  $t$  in lattice units (a factor of  $(12/16)^{3/2}$  has been included for the U395 12 data set). The continuous (dotted) straight lines represent fits to the expected behaviour for U355 (C410) and their slopes ( $xa$ ) are related to the effective coupling constant  $\bar{g}$  as described in the text.

able for an S-wave decay at threshold. We now explore hybrid meson decays.

#### D. Hybrid meson decay

With our lattice parameters, there are several two-body thresholds with the quantum numbers of the hybrid meson in the energy range of interest, namely  $\pi f_1$ ,  $\pi b_1$ ,  $\pi\eta$  and  $\pi\rho$ , where the latter two cases involve non-zero momentum since they are P-wave decays. We first investigate the coupling between the hybrid meson  $\hat{\rho}$  and the two-body channel  $\pi b_1$ . This latter channel has an S-wave coupling to the hybrid, so the energy threshold on our lattice is given by the values of  $aE(\pi, b_1)$  in Table III. These values are similar to our estimate of the hybrid meson mass, so that the normalised off-diagonal transition gives useful information. We use similar methods for  $\hat{\rho} \rightarrow b_1\pi$  as used above for  $b_1 \rightarrow \pi\omega$ .

The simplest way to investigate the hadronic matrix element responsible for decay  $\hat{\rho} \rightarrow b_1\pi$  is to evaluate the

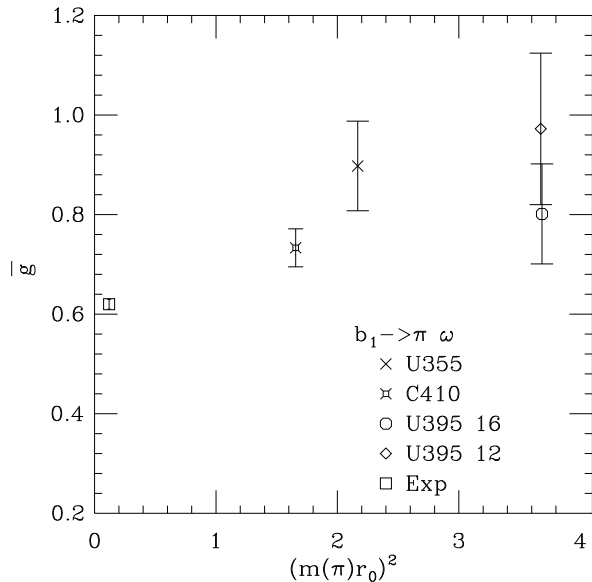


FIG. 3: Effective coupling of transition  $b_1 \rightarrow \pi\omega$  evaluated from the slope in fig. 2 at time  $t/r_0 = 1$  for different lattices with different pion masses (in units of  $r_0 \approx 0.5$  fm). The strange quark mass corresponds to  $(m(\pi)r_0)^2 \approx 3.4$ .

Code	$\hat{\rho} \rightarrow b_1\pi$		$\hat{\rho} \rightarrow f_1\pi$	
	$xa$	$\Gamma/k$	$xa$	$\Gamma/k$
U355	1.07(2)	0.046(5)	0.58(12)	0.017(7)
C410	1.60(4)	0.045(7)	0.82(26)	0.023(7)
Average		0.66(20)		0.15(10)

TABLE III: Hybrid meson decay amplitudes and rates.

ratio

$$H(t) = \frac{(\hat{\rho}|b_1\pi)}{\sqrt{(\hat{\rho}|\hat{\rho})(b_1|b_1)(\pi|\pi)}}$$

where each correlation is taken at the same  $t$ -separation on the lattice. This ratio normalises the meson creation operators. One could also normalise directly the two-particle state ( $\pi b_1$ ) but, as discussed [18] for  $\rho \rightarrow \pi\pi$ , we expect the dominant contribution to be the product (especially for large  $L$ ). Indeed we do check that the correlation between these two-point correlators ( $\pi|\pi$ ) and ( $b_1|b_1$ ) is consistent with zero out to  $t = 8a$ .

If there were only a single state coupling to the  $\hat{\rho}$  and  $\pi b_1$  operators, the ratio  $H$  would be 1.0. The observed value is small (see fig. 4) which shows that this is not the case.

In the case where there are two states (the hybrid me-

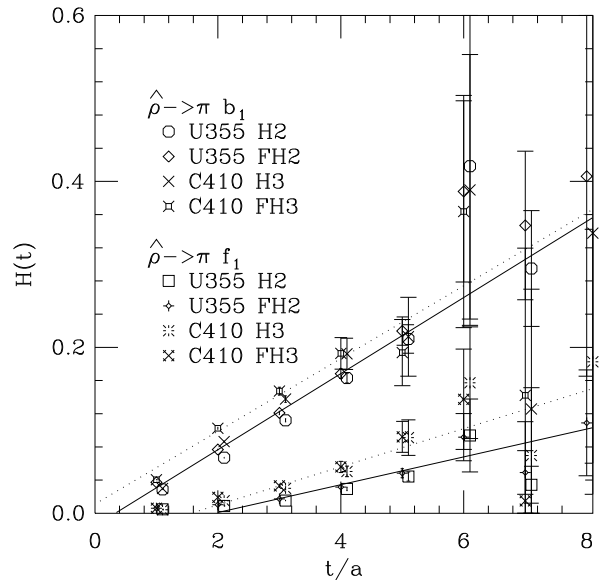


FIG. 4: Normalised ratio of  $\hat{\rho} \rightarrow b_1\pi$  and  $\hat{\rho} \rightarrow f_1\pi$ . The operator used for  $\hat{\rho}$  is either U-bends of size 2 or 3 (H2 or H3) or the same combined with fuzzing (FH2 or FH3). The  $\pi$  and axial meson are always fuzzed. The straight lines represent the trend of the data: the slope ( $xa$ ) is the quantity required.

son and the two-body threshold), the ratio  $H(t)$  then behaves [1] as  $xt$  where  $x$  is the lattice transition amplitude, provided that the transition is approximately on-shell and that  $xt \ll 1$ . We do indeed observe an approximately linear behaviour and, moreover, the value is consistent between different choices of external operator (fuzzed or not) for both the  $b_1$  meson and the  $\hat{\rho}$ . Thus we can assume that the ground state mesons dominate and read off the lattice transition amplitudes which are given in Table III. Statistically these slopes are quite well determined, although as we discuss later, the systematic errors are dominant. The decay width  $\Gamma$  is given, via Fermi's Golden Rule, by

$$\Gamma/k = \frac{1}{\pi}(xa)^2(L/a)^3 \frac{E(b_1)aE(\pi)}{E(b_1) + E(\pi)}$$

where  $k$  is the centre of mass momentum of the decay products.

Then using our observed mass values for the  $\pi$  and  $b_1$ , the values we obtain for the partial width  $\Gamma/k$  of the decay  $\hat{\rho} \rightarrow b_1\pi$  are given in Table III. We emphasise that, on the lattice, we are working with unphysical light quark masses which makes the transition nearly on-shell. The underlying assumption, however, is that the coupling constant  $g$  (where  $\Gamma/k$  is an effective proxy for  $g^2$ )

is insensitive to changes in the quark masses. This was confirmed by our study [18] of  $\rho$  decay and our study, above, of  $b_1$  decay shows only a relatively small dependence (see fig. 3).

As shown in Table III, the resulting values of the coupling (quoted as  $\Gamma/k$ ) vary between the two lattice evaluations we have used. As discussed above for  $b_1$  decay, each set of lattice configurations has favourable and less favourable features (large volume, smaller lattice spacing, lighter quarks, etc.). The best way forward is to regard these two studies as indicative of the systematic errors arising from these limitations. As a compromise we quote averaged effective couplings in Table III which take into account some of these systematic errors.

As well as  $\hat{\rho} \rightarrow \pi b_1$ , we can also explore another S-wave decay:  $\hat{\rho} \rightarrow \pi f_1$ . In this case, a disconnected diagram also contributes to the decay, but we expect the contribution from such disconnected diagrams to be small for the axial-vector meson [32]. We also assume that the  $f_1$  meson, because of the small disconnected contribution, is dominantly  $\bar{u}u + \bar{d}d$ . Then the relevant ratio is shown also in fig. 4. This again shows a linear increase with  $t$ , leading to estimates of the hadronic transition  $xa$  and partial width  $\Gamma/k$  for this decay shown in Table III. These substantially smaller values are only partly attributable (a factor 0.5 in rate) to quark diagram counting and are dominantly a dynamical effect.

If one was convinced that the disconnected contributions could be neglected for  $\hat{\omega}$  decays to  $\pi a_1$  then our estimate for  $x$  obtained above can be used. With the same assumptions we would obtain a partial width  $\Gamma/k$  of 0.45(30).

The excited two body state where  $\pi$  and  $b_1$  have momenta  $\pm 2\pi/L$  has an energy estimated on our U355 lattice at  $Ea = 1.36$ . This is close to the energy we find for our hybrid state. It would be desirable to evaluate the transition from  $\hat{\rho}$  to this excited two-body state to check for a consistent estimate of the decay width. On a lattice, however, this excited two-body state will be very hard to isolate because of the dominant contribution of the threshold state which has the same overall quantum numbers.

In this work we do not explore the P-wave decay channels such as  $\pi\rho$ ;  $\pi\eta$  etc., since we have not introduced non-zero momentum, although as in the case of  $\rho$  decay, this is in principle possible.

With  $N_f = 2$  flavours of sea-quark, we expect the  $\hat{\rho}$  meson to be mixed with the two body channels such as  $\pi b_1$ . Indeed by careful measurement of the energy of the two-body state, it is possible to deduce [26, 27, 28, 29] the scattering phase shift and, hence, properties of the  $\hat{\rho}$  resonance, if there is only one two-body channel open. In this case, however, several channels are open which invalidates the assumptions. Furthermore, we do not have sufficient precision in our energy determination to pursue this although preliminary attempts have been made [33].

We can, however, attempt a joint fit to the matrix

of operators available: three  $\hat{\rho}$  operators (as discussed above) and also the  $\pi b_1$  operator where the  $\pi$  is fuzzed but the  $b_1$  may be either local or fuzzed. We thus have a  $4 \times 5$  matrix of correlations, assuming that  $(\pi b_1 | \pi b_1)$  can be replaced by the product  $(\pi | \pi)(b_1 | b_1)$  which we do measure. For U355, from such a 3-state fit for the  $t$ -range 4-8 we obtain lowest energies of 0.93(15)/ $a$  and 1.41(8)/ $a$ . This is indeed consistent with the picture we have assumed so far.

### III. DISCUSSION

We study the spin-exotic channel with  $J^{PC} = 1^{-+}$  and we do obtain a signal for a state additional to the two-body threshold. On our lattices this state is relatively heavy - at 2.2(2) GeV. We find consistent mass values from the hybrid channel alone and when the  $\pi b_1$  channel is included. Since mixing between the discrete two-body channels and the hybrid meson is enabled on our lattice, it is possible that this mixing moves the hybrid mass up - but this shift would be expected to be of order  $xa$  which we find to be only 0.05 and hence within our quoted statistical error. As we only have a signal out to  $t/a \approx 6$ , we will not be able to resolve a rich hybrid spectrum - since we are only able to make 2-state fits to the hybrid sector. So it is possible that there are several hybrid mesons in this mass region, one of which is lighter than our mass estimate. Indeed our variational estimate explicitly is an upper mass estimate. We do have some control over the contribution of two-body states to the hybrid sector and those we explicitly measure contribute only a negligible amount.

For our quark masses (approximately 2/3 of strange for U355 and 1/2 for C410), previous lattice results gave a lighter hybrid mass (around 2 GeV), but they were predominantly quenched. We do not attempt a mass extrapolation, although phenomenological estimates [2, 3] would be that the light-quark hybrid state is some 200 MeV lighter than that we study here. For further discussion of the subtleties of extrapolating in quark mass see ref. [5, 34]. We are also unable to extrapolate to smaller lattice spacing or to larger spatial volumes. The neglect of strange sea-quarks is also hard to quantify but could be quite small for the states we consider. Even though these restrictions imply that our mass determination has systematic errors, we are considering a consistent lattice field theory and we expect hadronic transition strengths to be a good indication of the physical world.

The signal for the hadronic transition which causes decay is very clear and is consistent with the simple interpretation in which the slope gives the decay amplitude. The most suitable way to quote our result is as effective couplings given by partial widths  $\Gamma(\hat{\rho} \rightarrow \pi b_1)/k = 0.66(20)$  and  $\Gamma(\hat{\rho} \rightarrow \pi f_1)/k = 0.15(10)$ . These error estimates do not include any error from extrapolation to physical quark masses. If the  $\hat{\rho}$  meson is at 2.0 GeV then the physical decay to  $\pi b_1$  has momentum  $k = 0.611$  MeV

and for a heavier hybrid meson the momentum would be even larger. This implies that we expect the hybrid meson to have a partial width to  $\pi b_1$  of 400(120) MeV which implies a total width greater than this.

There are experimental indications for a  $\hat{\rho}$  resonance around 2 GeV with a total decay width reported as 333 MeV (from ref. [15] studying  $\pi f_1$  final states) and as 230 MeV (from ref. [16] studying  $\pi b_1$  final states). These total width values should be the same if there is one underlying state and can be compared with the total width we estimate. The agreement is close enough to warrant further experimental investigation. It would be of considerable interest to know if the experimental branching fractions (as yet unknown) tie in with our expectation (namely dominance of  $\pi b_1$  over  $\pi f_1$ ). Indeed phenomenological models do indicate [34] that the  $\pi b_1$  mode should dominate the width and that widths of  $O(100)$  MeV are possible. Flux tube models [35, 36] give  $\Gamma/k$  in the range .06 to .28 for  $\pi b_1$  and .04 to .10 for  $\pi f_1$ .

The equivalent decay to  $\hat{\rho} \rightarrow \pi b_1$  for a heavy-quark hybrid will be  $\hat{Y} \rightarrow B(0^-)B^{**}(1^+)$  which is not expected to be allowed energetically. So the previous estimate [1] for the decay width of the  $\hat{Y}$  is not modified by this work.

#### IV. CONCLUSIONS

We have evaluated the S-wave transition  $b_1 \rightarrow \pi\omega$  at threshold from the lattice and obtained agreement with the experimental value. We find some evidence that the coupling constant varies with the quark mass, being smaller for lighter quarks.

We have studied the spectrum and decay to  $\pi b_1$  and  $\pi f_1$  of the spin exotic isovector hybrid meson  $\hat{\rho}$ . This state has potential couplings to many two-body states in the same energy region which inevitably means that approximate methods will be needed. We find statistically well determined results in our study which are consistent with a hadronic transition from  $\hat{\rho}$  to  $\pi b_1$  and  $\pi f_1$  whose strength we evaluate. From this lattice determination, assuming that the effective coupling constant is independent of quark mass, one can estimate the physical partial widths, obtaining  $\Gamma(\hat{\rho} \rightarrow \pi b_1)/k = 0.66(20)$  and  $\Gamma(\hat{\rho} \rightarrow \pi f_1)/k = 0.15(10)$  where  $k$  is the decay momentum. Note that, if the result we found for  $b_1 \rightarrow \pi\omega$  is generic and the effective coupling decreases with quark

mass, then the physical decay width of the hybrid meson would be smaller than our estimates. We note that the width of the hybrid meson is large primarily because of larger phase space rather than larger coupling, compared to the decay of a typical meson, such as  $b_1 \rightarrow \pi\omega$ .

Our determination of the mass of this hybrid meson gave higher values than obtained previously for our lattice with smaller lattice spacing (U355) but averaging over our two sets of lattices we obtain 2.2(2) GeV for light quarks of similar mass to strange, which is similar to the value 2.0(2) GeV previously determined. Because of the possibility of a rich spectrum (both of hybrid mesons and of two-body states) we cannot exclude systematic errors in our mass determination and we can only be certain that it is an upper limit. We do, however, see some evidence that the hybrid meson may lie higher in energy when the two-body decay channels are coupled (as they are with dynamical sea quarks).

The study of the properties of an unstable state (namely the spin-exotic hybrid meson) demands careful treatment on a lattice. We have shown that this is feasible and future studies with lattices closer to the continuum and with lighter quarks and higher statistics will allow further refinement of our estimates.

Overall our results are rather disappointing from a viewpoint of experimental searches for spin-exotic hybrid mesons. We have evaluated two decay channels which combine to give a total width of over 400 MeV. This will make the detailed experimental study of the hybrid meson relatively difficult. There are detailed predictions (such as that the  $\pi b_1$  mode will be dominant) that can be checked, however.

#### V. ACKNOWLEDGEMENTS

One of the authors (CM) wishes to thank PPARC for the award of a Senior Fellowship. This work has been supported in part by the EU Integrated Infrastructure Initiative Hadron Physics (I3HP) under contract RII3-CT-2004-506078. We acknowledge the ULGrid project of the University of Liverpool for making available computer resources. We acknowledge the CP-PACS collaboration [24] for making available their gauge configurations.

---

[1] UKQCD, C. McNeile, C. Michael, and P. Pennanen, Phys. Rev. **D65**, 094505 (2002), hep-lat/0201006,  
 [2] UKQCD, P. Lacey, C. Michael, P. Boyle, and P. Rowland, Phys. Rev. **D54**, 6997 (1996), hep-lat/9605025,  
 [3] UKQCD, P. Lacey, C. Michael, P. Boyle, and P. Rowland, Phys. Lett. **B401**, 308 (1997), hep-lat/9611011,  
 [4] MILC, C. W. Bernard *et al.*, Phys. Rev. **D56**, 7039 (1997), hep-lat/9707008,  
 [5] J. N. Hedditch *et al.*, Phys. Rev. **D72**, 114507 (2005),

hep-lat/0509106,  
 [6] TXL, P. Lacey and K. Schilling, Nucl. Phys. Proc. Suppl. **73**, 261 (1999), hep-lat/9809022,  
 [7] C. Bernard *et al.*, Phys. Rev. **D68**, 074505 (2003), hep-lat/0301024,  
 [8] IHEP-Brussels-Los Alamos-Annecy(LAPP), D. Alde *et al.*, Phys. Lett. **B205**, 397 (1988),  
 [9] E852, D. R. Thompson *et al.*, Phys. Rev. Lett. **79**, 1630 (1997), hep-ex/9705011,

- [10] Crystal Barrel, A. Abele *et al.*, Phys. Lett. **B423**, 175 (1998),
- [11] E852, G. S. Adams *et al.*, Phys. Rev. Lett. **81**, 5760 (1998),
- [12] E852, S. U. Chung *et al.*, Phys. Rev. **D60**, 092001 (1999), hep-ex/9902003,
- [13] E852, E. I. Ivanov *et al.*, Phys. Rev. Lett. **86**, 3977 (2001), hep-ex/0101058,
- [14] A. R. Dzierba *et al.*, (2005), hep-ex/0510068,
- [15] E852, J. Kuhn *et al.*, Phys. Lett. **B595**, 109 (2004), hep-ex/0401004,
- [16] E852, M. Lu *et al.*, Phys. Rev. Lett. **94**, 032002 (2005), hep-ex/0405044,
- [17] C. Michael, PoS **LAT2005**, 008 (2005), hep-lat/0509023,
- [18] UKQCD, C. McNeile and C. Michael, Phys. Lett. **B556**, 177 (2003), hep-lat/0212020,
- [19] UKQCD, M. Foster and C. Michael, Phys. Rev. **D59**, 074503 (1999), hep-lat/9810021,
- [20] J. Foley *et al.*, Comput. Phys. Commun. **172**, 145 (2005), hep-lat/0505023,
- [21] UKQCD, P. Lacock, A. McKerrell, C. Michael, I. M. Stopher, and P. W. Stephenson, Phys. Rev. **D51**, 6403 (1995), hep-lat/9412079,
- [22] C. Michael, Int. Rev. Nucl. Phys. **9**, 103 (2003), hep-lat/0302001,
- [23] UKQCD, C. R. Allton *et al.*, Phys. Rev. **D65**, 054502 (2002), hep-lat/0107021,
- [24] CP-PACS, A. Ali Khan *et al.*, Phys. Rev. **D65**, 054505 (2002), hep-lat/0105015,
- [25] UKQCD, C. R. Allton *et al.*, Phys. Rev. **D60**, 034507 (1999), hep-lat/9808016,
- [26] M. Luscher, Commun. Math. Phys. **104**, 177 (1986).
- [27] M. Luscher, Commun. Math. Phys. **105**, 153 (1986).
- [28] M. Luscher, Nucl. Phys. **B354**, 531 (1991),
- [29] M. Luscher, Nucl. Phys. **B364**, 237 (1991),
- [30] Particle Data Group, S. Eidelman *et al.*, Phys. Lett. **B592**, 1 (2004),
- [31] T. Barnes, AIP Conf. Proc. **717**, 625 (2004), hep-ph/0311102,
- [32] UKQCD, C. McNeile, C. Michael, and K. J. Sharkey, Phys. Rev. **D65**, 014508 (2002), hep-lat/0107003,
- [33] M. S. Cook and H. R. Fiebig, PoS **LAT2005**, 062 (2005), hep-lat/0509028,
- [34] A. W. Thomas and A. P. Szczepaniak, Phys. Lett. **B526**, 72 (2002), hep-ph/0106080,
- [35] N. Isgur, R. Kokoski, and J. Paton, Phys. Rev. Lett. **54**, 869 (1985),
- [36] F. E. Close and P. R. Page, Nucl. Phys. **B443**, 233 (1995), hep-ph/9411301,